ISSN : 3105-0794

الهيئة الليبية للبحث العلمي

Libyan Authority For Scientific Research

(LIJNS) Libyan International Journal of Natural Sciences

VOLUME 2 ISSUE 1 MAY 2026

Bi-Annual, Peer- Reviewed, and Open Accessed e-Journal

DOLJ Directory of Online Libyan Journals

turnitin

Google Scholar

Puplished by

MILJS@aonsrt.ly

Libyan International Journal of Natural Sciences (LIJNS)
Vol.2 Issue No 1 May 2026

Kinetics and Equilibrium Studies of Methylene Blue Adsorption onto Cement Kiln Dust

Fateemah M. Rasheed*[1], Thiheeba K. Mansour[2], Fathi M. Jubran[3]
[1,2] Department of Zoology, Faculty of Science Nature Resources, AL-Jafara University, Libya.
[3] High Institute of Sciences and Technology, AL-Khomes, Libya.

ARTICLE INFORMATION

Article history:
Received 10 December 25
Accepted 5 February 26

Published 12 February 26

Keywords:
Adsorption, Methylene Blue Dye, Batch Mode Adsorption, Cement Kiln Dust.

ABSTRACT

This study examines the use of cement kiln dust (CKD) waste as an adsorbent for removing methylene blue (MB) dye through a batch-mode adsorption technique. The effect of some physical parameters, such as initial concentration of MB dye, mass of CKD adsorbent, and contact time, was considered. As a result, the optimal contact time was found to be 15 min for 95.35% removal of MB dye, the initial concentration of MB dye was 70 mg/l, and the mass of CKD adsorbent was equal to 0.10 g. The equilibrium data were analyzed using the Langmuir and the Freundlich isotherm models. The Langmuir isotherm model was found to fit the equilibrium data very well, with (R^2) equal to 0.982 for the adsorption of MB, and the adsorption capacity was 34.48 mg/g. The adsorption kinetics were found to follow the pseudo-second-order rate kinetic model, with a good correlation (R^2) equal to 0.988 for MB. This refers to the fact that the rate-limiting step was a chemosorption type of adsorption. The results showed that the CKD waste was found to be an attractive, low-cost adsorbent for the treatment of wastewater.

1. Introduction

Human and industrial activities have significantly contributed to the pollution of the environment. The continuous discharge of dye wastewater from factories, such as paper printing, paints, plastics, and agricultural fertilizers, as well as leather and textile tanning plants, has become a major source of environmental concern and a global problem for environmentalists. Leather and textile tanneries are among the largest consumers of water during processing and manufacturing, and so, they discharge enormous quantities of wastewater containing dyes [1].

Due to the random discharge of wastewater by some manufacturing facilities into open lands, rivers, and lakes, surface water and groundwater are often contaminated with hazardous substances. These substances can cause the depletion of dissolved oxygen (DO) in the water, which, in turn, contributes to the harm and death of aquatic organisms [2]. Most dyes are characterized by being carcinogenic and mutagenic substances, while exhibiting inertia and a lack of biodegradability for very long periods. They can also bioaccumulate within the living cells of host organisms (humans/animals), through the food chain, causing health risks [3, 4].

Manufacturing facilities face significant challenges in their own wastewater treatment. Primarily, the cost of efficient, advanced technologies and the need to treat limited pollutants, which sometimes requires specialized treatment. Fortunately, alternatives to these challenges always exist, including the use of cost-effective and efficient treatment systems and sustainable technologies presented in water reuse [5]. Innovative techniques in this regard include: Photodegradation, Biological Degradation, Ion exchange, Reverse osmosis, Electro-dialysis, Chemical reduction, Coagulation, and Adsorption [5-11].

Many studies and research papers emphasize the success of adsorption techniques in removing dyes using adsorbent surfaces made of inexpensive and effective materials, for instance: (a) food industry waste such as: date pits, olive pits, spent tea leaves, spent coffee grounds, and orange peels [12-17], (b) agricultural residues and wastes such as: barley straw, acacia leaves (*Acacia nilotica* L.), and pine leaves [18-20], (c) earth components such as zeolite [21], clays such as bentonite, and kaolin [22, 23], (d) solid industrial wastes such as: fly ash, steel slag, and CKD [24-26]. The last is a solid industrial waste product emitted incidentally during cement manufacturing processes and is traditionally released into the atmosphere. Environmentalists classify the cement industry and its by-products as polluting industries that directly harm public health [27, 28].

Scientific studies have not adequately evaluated the effectiveness of CKD as an adsorbent for removing dye substances from wastewater. The question that arises from this study: How can we provide treated water that is free of dyes and complies with Libyan standards and specifications using sustainable solutions? This study aims to evaluate the feasibility and capability of batch mode adsorption in

* Corresponding author: *E*-mail addresses: fateemahmahmoud34@gmail.com

removing dyes from their aqueous solutions, as well as the effect of some physical factors, such as the initial concentrations of MB dye, the mass of CKD adsorbent, and finally, the contact time on the adsorption process.

2. Methodology

2.1 Chemicals and Reagents

All chemicals used in this study were analytical grade reagents and used without any additional processing. The main chemical of the MB dye was of an analytical grade of < 98.0% purity, commercially obtained from Merck, in Germany. This was used to prepare the main solution and other standard solutions of varying concentrations of the MB dye. The adsorbent, consisting of CKD waste, was obtained from a Libyan cement plant, specifically, the Lubda plant located in Al-Khumms city in western Libya. It was collected from one of the plant's air pollution control units and placed in clean plastic bags.

2.2 Instruments and Tools

In this study, several instruments and tools were used, including a Fourier transform infrared (FTIR) spectrometer (Shimadzu, model IR Tracer-100 Kayto, made in Japan). It was used to identify the functional groups on the surface of CKD adsorbent before and after the adsorption process of MB dye, in the range of (400 – 4000) cm^{-1}. A Total Reflection X-Ray Fluorescence (TR-XRF) Spectroscopy, (A PicoTAX, Roentec model, made in Germany). It was used to measure the basic structures of minerals and provide quantitative or semi-quantitative results of the CKD adsorbent. A UV/VIS spectrophotometer (type UV-Analytikjena K, model 205 Specord). It was used to measure the concentrations of MB dye molecules at a wavelength (λ) of approximately 665 nm. A pH meter device (type 740 Inolab, WTW model) was also used. A dual electrode (SenTix 20) was also among the instruments utilised. The pH meter device was calibrated with a buffer solution to measure the pH of the solutions under study. For studying batch adsorption processes, a digital shaker device (model GFL 3005, made in Germany) was used. A sensitive Sartorius competence balance (model CP224S, made in Germany), with a maximum reading of 220 g and a minimum reading of approximately 0.001 g, was also employed. Finally, a set of stainless-steel sieves with various mesh sizes, and a variety of glassware, including standard 1-liter flasks, 250 ml conical flasks, suction tubes, and other apparatus, were used.

2.3 Description of CKD Adsorbent

Chemically, CKD particles are basic materials. Based on texture, they are fine and dry, which makes them highly absorbent. The particle size varies depending on the cement manufacturing process. Dust collected from dry kilns is smaller than that from wet and semi-wet/semi-dry processes [28]. The diameters of these particles range from (0.3 - 9.3) μm, depending on the manufacturing process. The most common primary components present in quantities greater than 5.0% in CKD particles are SiO_2, CaO, CO_3^{-2}, and K_2O [29-31]. On the other hand, the minor components, which constitute less than 5.0%, represent varying concentrations of hazardous organic compounds and heavy metals such as lead (Pb), cadmium (Cd), selenium (Se), and some radionuclides [32, 33].

2.4 Description of MB dye

Chemically, MB is known as a 3,7-bis(dimethylamino)-phenothiazine-5-ium chloride cation, has a chemical formula $C_{16}H_{18}N_3SCl$, a molecular weight of 319.85 g/mole, and a maximum absorption at a wavelength (λ) of 665 nm [34]. This dye was used in this study as a model compound of basic dyes in particular, and as an organic compound in general (Figure 1).

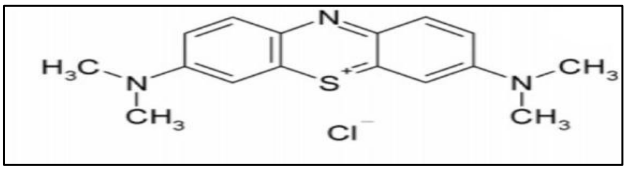

Fig. 1: Chemical structure of MB dye molecule [34].

3. Study Methods

3.1 Preparation of the CKD Adsorbent

CKD is a byproduct of cement manufacturing processes. The gases emitted from the rotary kiln chimneys of the plant often carry large quantities of this dust. Typically, the dust is filtered using special filters installed in the plant chimneys [32]. This heterogeneous dust, varying in particle size, is collected and subsequently ground and sieved in the laboratory to a very fine size (1.0 – 5.0) μm, to obtain a homogeneous particle size suitable for use in this range. The collected CKD is dried in the kiln at 105 °C for 24 hours. The final step involved storing the dried sample in a glass desiccator to protect it from moisture until the time of use.

3.2 Preparation of Standard Solutions of MB dye

(1) The stock solution of 1000 mg/l MB is prepared by dissolving the weighted amount of dye in distilled water with thorough stirring and shaking. The dissolved amount is transferred to a 1.0 L standard flask, and the volume is topped up to the mark with distilled water.
(2) Solutions of MB with different concentrations (10, 30, 50, 70, 100, 150, 200) mg/l are prepared by diluting the stock solution to the appropriate concentration.

3.3 Batch mode adsorption process

The adsorption process is performed using a digital shaker at a room temperature of (26 ± 2) °C, a pH of 6.5, a shaking rate of 200 rpm, for varying contact times (5, 10, 15, 30, 60) min. Using 250 ml conical flasks, all adsorptions are carried out by mixing different masses of CKD adsorbent (0.05 – 0.30) g with different solutions containing initial concentrations of MB dye (10, 30, 50, 70, 100, 150, 200) mg/l in a fixed solution volume of 50 ml. In this study, the effect of several physical variables, such as initial MB dye concentrations, CKD adsorbent masses, and contact times, on the adsorption process was evaluated.

3.3.1 Testing the Effect of MB Concentration

The effect of this variable is investigated by weighing a fixed quantity of CKD (0.20 g is chosen preliminary as optimal) and adding it to 50 ml of MB dye solution on several occasions, each time at a different concentration (10, 30, 50, 70, 100, 150, 200) mg/l at a shaking rate of 200 rpm for 15 min at room temperature (26 ± 2) °C and a pH of 6.5.

3.3.2 Testing the Effect of CKD Adsorbent Mass

The effect of this variable is investigated by adding 50 ml of MB dye solution at a concentration of 100 mg/l (previously selected as optimal) to varying amounts of CKD (0.05 – 0.30) g at a shaking rate of 200 rpm for 15 min. at room temperature (26 ± 2) °C and pH 6.5.

3.3.3 Testing the Effect of Contact Time

The effect of contact time is also investigated at different times (5, 10, 15, 30, 60) min by weighing a fixed amount of CKD equaled to 0.20 g (The best quantity tested in a previous test) and added to 50 ml of MB dye solution at the best concentrations tested previously, which is 100 mg/l, at a shaking rate of 200 rpm, room temperature of (26 ± 2) °C and a pH of 6.5.

4. Measurement Method

After the adsorption process is completed, the content of each conical flask is filtered, and the adsorbent is removed and separated using Whatman filter paper. The residual concentration of MB in each conical flask is determined using a UV/VIS spectrophotometer, and the amount of adsorption at equilibrium (q_{eq}), expressed in mg/g, is calculated as follows [35]:

$$q_{eq} = [\ (C_0 - C_e) * V\ ]\ / W \quad (1)$$

Where: (C_0) and (C_e) (mg/l) represent the initial and final concentrations of MB at the beginning and end of the adsorption process, respectively; (V) represents the volume of MB solution, measured in liters; and (W) represents the mass of CKD adsorbent, measured in grams. However, the adsorption percentage (%) is estimated as follows [35]:

$$\%\ Adsorption = [\ (C_0 - C_e) / C_0\ ] * 100 \quad (2)$$

5. Results and Discussion

5.1 Adsorbent Properties

Generally, CKD, like other solid dust residues, contains primary components present in quantities greater than 5%, such as SiO_2, CaO, CO_3^{-2}, K_2O, SO_4^{-1}, and Cl^{-1} [29 - 31]. For example, in the United States, several CKD samples from various raw cement sources were analyzed, and it was confirmed that all contained CaO at a rate of (38 – 63)%, total alkali metals between (2 – 11)%, SO_4^{-1} between (3 – 17)%, and MgO between (1 – 25)%. This report indicated that 50% to 90% of CKD had particles with diameters less than 10 µm, making it a harmful substance to human health, as it falls within the range of particles that can be inhaled through the respiratory system. In this study, the particle size of the dust after manual grinding, drying, and sieving was between (5 - 10) µm. Therefore, masks are required during laboratory tests as a precautionary measure.

A sample of CKD is analyzed using Total Reflection X-ray fluorescence (TR-XRF) spectroscopy, and the specific compositions are shown in Table 1.

Table 1: Chemical Composition of CKD by (TR-XRF) spectroscopy.

Serial Number	Chemical Composition Name	Quantity (%)
1	Calcium oxide CaO	70.9
2	Silica SiO_2	7.28
3	Ferric oxide Fe_2O_3	4.3
4	Alumina Al_2O_3	3.14
5	Magnesium oxide MgO	1.29
6	Potassium oxide K_2O	0.51
7	Titanium oxide TiO_2	0.22
8	Phosphorus oxide P_2O_5	0.11
9	Sulfur oxide, SO_3	0.09
10	Chlorides, Cl^-	0.07
11	Manganese oxide MnO	0.05

(TR-XRF) The spectroscopy results in Table 1 show that the primary component of the studied dust is CaO, comprising 70.9 % by weight. SiO_2 is also present at 7.28%. The remaining components consist of Fe_2O_3 with 4.3% and Al_2O_3 with 3.14%.

5.2 FTIR analysis

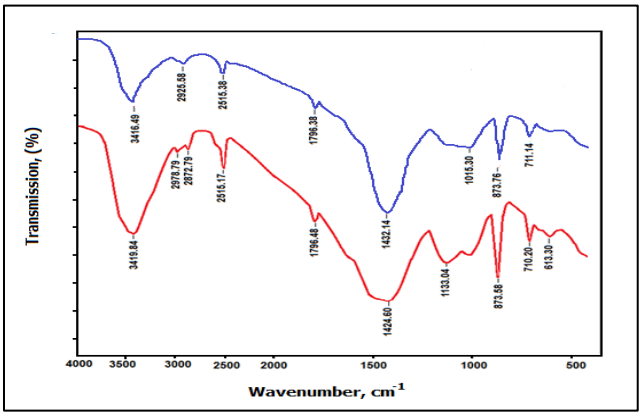

Fig. 2: FTIR spectra of CKD adsorbent before (Bottom) and after MB dye removal (Top).

In Figure 2, the FTIR spectra of the CKD adsorbent were conducted before (The bottom spectrum with red color) and after the adsorption (The top spectrum with blue color) of the MB dye from its aqueous solutions. This spectrum shows both stretching and bending vibration types of bands involved in the molecular structure of the CKD adsorbent. In the CKD FTIR spectrum, it can be seen that the broad band at a wavenumber equal to 3421.38 cm^{-1} is ascribed to the O–H stretching vibrations type of bands in minerals [36, 37]. While the absorption bands at the wavenumber equaled to 2978.79 and 2872.79 cm^{-1} may be attributed to C-H stretching vibrations in alkanes [38]. However, the absorption bands at 1424.60 cm^{-1} and 873.58 cm^{-1} may be assigned to the presence of carbonate (CO_3^{2-}) group [39]. The

absorption bands positioned at 1133.04 cm^{-1} and 710.20 cm^{-1} may be attributed to the presence of silicate stretching vibration bands [40]. Finally, the wavenumber of 613.30 cm^{-1} may be related to K–O vibration bands [41]. In the top spectrum (Blue one), which belongs to the CKD after finishing the batch mode adsorption process, it can be seen that there are weakening, small shifts, and sometimes disappearances of some peaks in CKD bands, which are detected in the FTIR spectrum. In this way, the bonding of the MB dye onto CKD particles is strongly confirmed, as seen in Figure 3.

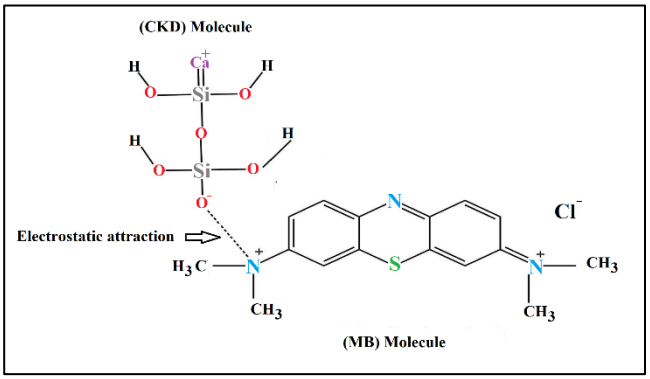

Fig. 3. Schematic representation of the adsorption mechanism of the MB dye molecule onto CKD particle surface [42].

5.3 Effect of the adsorption parameters

The various adsorption operating conditions, like concentration of MB dye, CKD mass, and contact time, are varied and optimized to attain the efficient adsorption of MB dye onto CKD.

5.2.1 Effect of Initial Concentrations of MB Dye

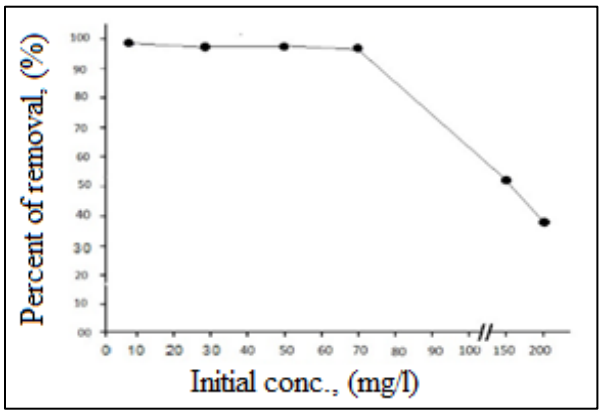

Fig. 4: MB dye Concentrations vs. the (%) removal of MB.

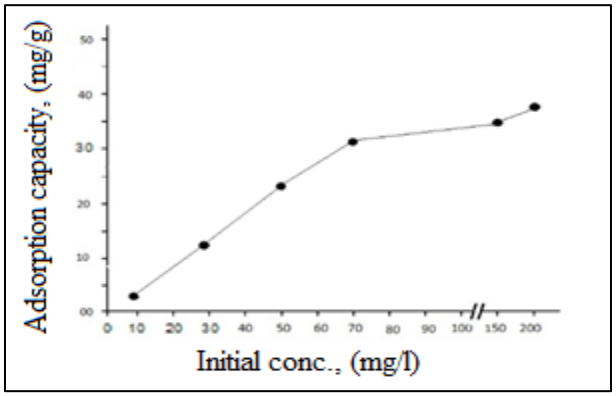

Fig. 5: MB dye Concentrations vs. the adsorption Capacity (q_{eq}) of CKD adsorbent at equilibrium.

From Figure 4, it is clearly observed that the removal rate of MB molecules increases from the start, and remains relatively constant up to an initial MB dye concentration of 70 mg/l. Subsequently, the removal rate of the dye in its aqueous solution decreases significantly from (95.35 – 43.79)% as its concentration increases from (>70 – 200) mg/l. Conversely, the amount of MB adsorbed per unit mass of adsorbent (q_{eq}) increased from (4.96 - 37.79) mg/g (Fig. 5) with increasing dye initial concentrations from (10 – 200) mg/l.

The high removal percentage (%) at low dye concentrations is attributed to the fact that all dye molecules present in the adsorption solution at these low concentrations interact with the freely available active sites, thus enabling a high removal percentage. Conversely, at higher concentrations, the active sites become saturated with dye molecules in the adsorption solution, resulting in saturation and a decrease in the removal percentage [43].

However, published scientific studies [43, 44] attribute the significant increase in the adsorption capacity (q_{eq}) of CKD to the fact that the initial concentrations of MB dye provide a substantial driving force to overcome the mass transfer resistance of MB dye molecules between the aqueous solution and the solid phase. The difference in adsorption capacity between various solid adsorbents depends on the differences in their surface properties and chemical compositions [46].

5.2.2 Effect of CKD adsorbent mass

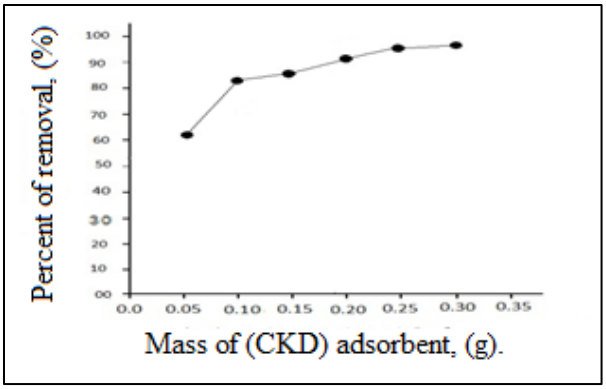

Fig. 6: CKD adsorbent mass vs. MB particles (%) removal.

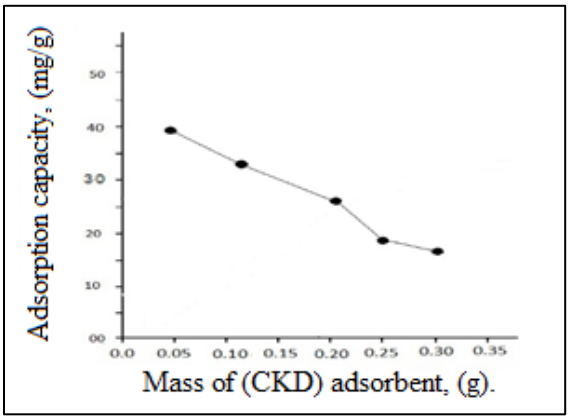

Fig. 7: Mass of CKD adsorbent vs. its adsorption capacity for different MB molecule concentrations.

Figure 6 illustrates the relationship between different masses of the CKD adsorbent, ranging from (0.05 - 0.30) g, and the percentage removal of MB dye molecules from its aqueous solution. In contrast, Figure 7 shows the relationship between different masses of the same adsorbent versus its adsorption capacity (q_{eq}) at equilibrium as it adsorbs the MB dye molecules from its aqueous solution.

The percentage removal (%) of MB dye molecules from its aqueous solution is obtained using a batch mode adsorption process under the operating conditions described previously. Initially, Figure 6 clearly shows the decrease in the concentration of residual MB dye molecules in the conical flask solution from (100 - 0.26) mg/l as the CKD mass increased from (0.05 - 0.30) g. With such an increase in CKD mass, the percentage removal of MB dye molecules increased from (69.57 - 97.63) %. Several published scientific reports attribute these results to the increase in the number of active sites available within the CKD particles for the adsorption of MB dye molecules, with an increase in the CKD mass from (0.05 - 0.3) g. This, in turn, causes an increase in the percentage removal of MB dye molecules [43, 44]. On the other hand, when calculating the adsorption capacity (q_{eq}) at equilibrium (using Equation (1)) of the CKD, it can be observed that the adsorption capacity (q_{eq}) of CKD for MB dye molecules was 38.66 mg/g when using 0.05 g of the adsorbent mass, and 11.65 mg/g when using 0.30 g of the same adsorbent mass. It is likely that the reduced abundance of active sites in the CKD during the adsorption of MB dye molecules, resulting from the entanglement and overlap of these active sites when the CKD mass increased from (0.05 - 0.30) g, contributed to the decrease in the adsorption surface area. This, in turn, led to a decrease in the amount of MB dye molecules adsorbed by the CKD adsorbents [45, 47].

5.3.4 Effect of Contact Time

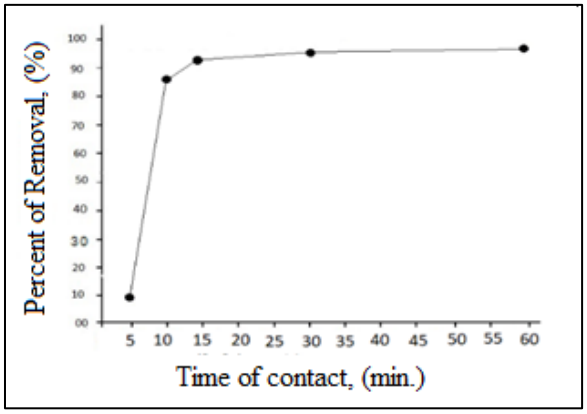

Fig. 8: Contact time vs. the (%) removal of MB dye molecules by CKD adsorbent.

Batch mode adsorption is performed at different contact times (5, 10, 15, 30, 60) min. The concentration of MB dye was 100 mg/l, while the mass of the CKD was 0.2 g. Figure 8 shows that the MB dye removal rate increases rapidly with increasing contact time up to 15 min. Subsequently, the adsorption process continues slowly until it gradually reaches an equilibrium state. At this point, it can be said that most of the active sites are occupied, and the process reaches a near-equilibrium state after 15 minutes under the operating conditions.

As previously reported, the adsorption rate is highest at the beginning of the adsorption process due to the larger surface area and the abundance of active sites in the CKD responsible for trapping the MB dye molecules [48, 49], in addition to the driving forces provided by the initial concentrations. These forces overcome the resistance of the MB dye's transition mass between the solution and the solid phase [50].

6. Isotherm Analysis

Two Isotherm Line Equations: Langmuir and Freundlich Models for the Adsorption of MB.

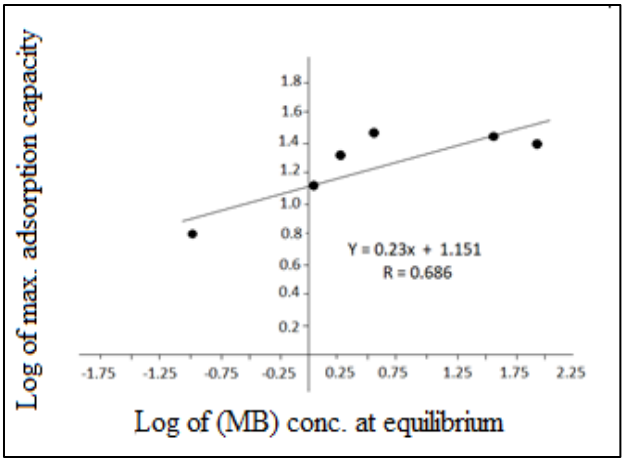

Fig. 9: Isotherm for the Freundlich Model of the Adsorption of MB dye molecules by CKD.

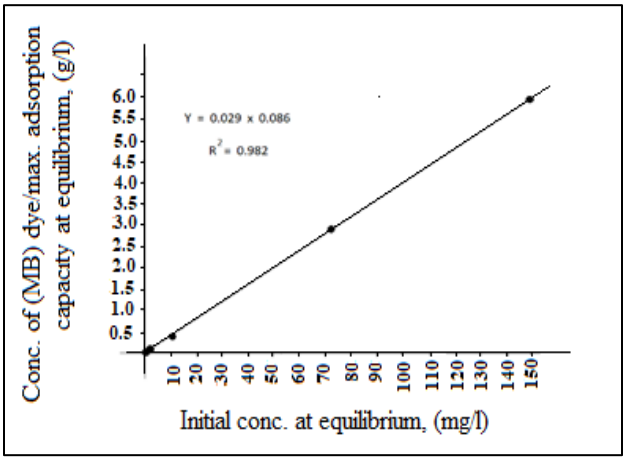

Fig. 10: Isotherm for the Langmuir Model of the Adsorption of MB dye by CKD.

Figures 9 and 10 show line graphs obtained from the relationship between the logarithmic (q_{eq}) and (C_e), as well as the relationship between the quotient (C_e/q_{eq}) and the equilibrium concentrations (C_{eq}) for the adsorption processes of MB dye.

For the Langmuir and the Freundlich models of isotherm line equations, the coefficient of determination (R^2) for each relationship was estimated to be approximately 0.982 and 0.686, respectively. The slope and intersection values, derived from the linear relationship, were used to calculate the constants in the aforementioned isotherm line equations.

Table 2 presents the data obtained from the isotherm line equations, representing the values of the constants for the Langmuir and the Freundlich models of the batch mode adsorption process of MB dye. Linear equations were used in Figures 9 and 10, which represent the relationship between the logarithmic values of (q_{eq}) and (C_e), as well as the relationship between the quotient of (C_e/q_{eq}) and the equilibrium concentrations (C_{eq}) for the adsorption processes.

Table 2: Results of the two-line equations of isotherm models: the Langmuir model and the Freundlich model for the adsorption of MB dye.

Langmuir Model			Freundlich Model		
q_{max} (mg/g)	K_L (l/mg)	R^2	K_f (l/g)	n (l/mg)	R^2
34.48	0.3372	0.982	14.158	4.329	0.686

Regarding the adsorption process of MB dye molecules, it can be observed that the constants of the isotherm line equations for the Freundlich model, representing the adsorption capacity (K_f), adsorption intensity, and validity (n), are estimated to be approximately 14.158 l/g and 4.329 l/mg, respectively. Meanwhile, the values of the Langmuir model's equilibrium constants, namely the maximum adsorption capacity (q_{max}) in mg/g and the active site attraction (K_L) in l/mg, are approximately 34.48 mg/g and 0.3372 l/mg, respectively.

The linear equations in Figures 9 & 10 for the adsorption process of MB molecules indicate that the coefficient of determination (R^2) of the Langmuir model is higher than that of the Freundlich model. This agreement with the Langmuir model suggests that the isotherm line equation provides a good model for the system.

7 Adsorption Kinetics Analysis

Pseudo-first-order and pseudo-second-order adsorption kinetics models

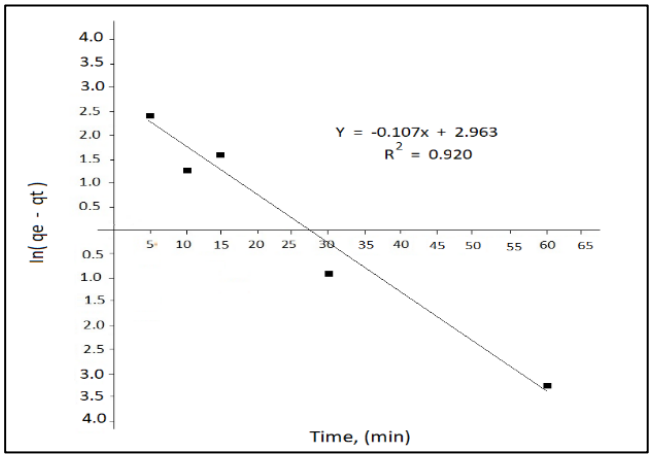

Fig. 11: Pseudo-first order adsorption kinetics model for MB dye.

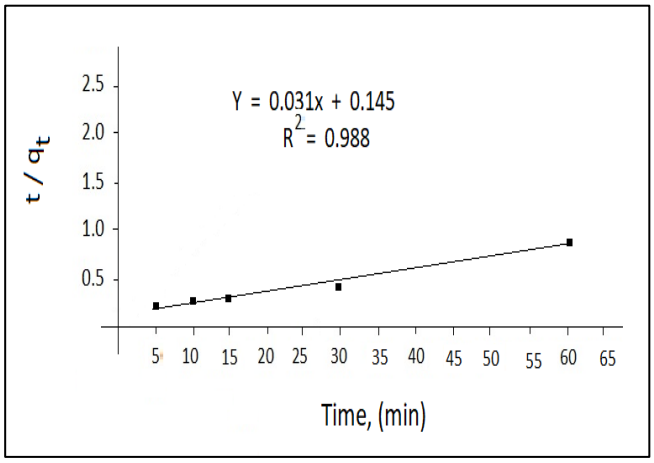

Fig. 12: Pseudo-second order adsorption kinetics model for MB dye.

Regarding the pseudo-first-order adsorption kinetics model, and based on the data in Table 3 and the kinetic equations, it can be observed that the coefficients of determination (R^2) for the pseudo-first-order adsorption kinetics model and the pseudo-second-order adsorption kinetics model for the adsorption of MB onto CKD adsorbent particles were 0.960 and 0.988, respectively. Therefore, it can be concluded that the results are very consistent with this model of quasi-second-order adsorption kinetics and that the maximum adsorption capacity values recorded in Table 3 for quasi-second-order adsorption kinetics of MB molecules are very close to what was obtained experimentally.

Table 3: Comparison between first-order and second-order adsorption kinetics results for the adsorption of MB molecules onto CKD adsorbent surfaces.

First-order adsorption kinetics			Second-order adsorption kinetics		
K (min^{-1})	Q (mg/g)	R^2	K (min^{-1})	q (mg/g)	R^2
0.107	14.776	0.920	0.00663	35.13	0.988

Once again, despite the previous conclusions mentioned in the "Contact Time Effect" section, and the two linear relationships (t) versus (t/qt), as well as (t) versus (In(qe – qt)) (Fig. 11) and (Fig. 12), and through the results recorded in Table 3, it is clear that the adsorption process of the dye molecules did not follow first-order kinetics, indicating that the adsorption process was not controlled by diffusion and that the adsorption progressed by diffusion across the membrane, as indicated in a previous report [51]. The pseudo-second-order kinetic model clearly shows an agreement with the slightly higher coefficient of determination (R^2) of approximately 0.988. This suggests that the rate-limiting step was a chemosorption mechanism (representing one of the adsorption mechanisms mentioned in a previous report [52]) arising from either valence forces through electron sharing between the adsorbent and the adsorbate, or covalent forces between them, as reported in a previous report [52]. The pseudo-second-order adsorption rate constant (K^2) and the adsorption capacity at equilibrium and at a specific time (q_e) were estimated by plotting the slope and the intersection point in the graph above, respectively. The estimated adsorption capacity (q_e), approximately 35.13 mg/g, also confirms agreement with the experimental results. The pseudo-second-order kinetic rate constant (K^2) for the CKD was approximately 0.00663 g/mg/min.

Conclusions

The results of the study led to several conclusions, most notably the role of CKD wastes in removing water coloring MB dye pollutant from its aqueous solution. In specific:

- Higher content of CKD adsorbent resulted in a higher removal percentage (%) of MB dye molecules from aqueous solution.
- Higher initial MB dye concentrations inversely impacted the removal percentage (%) of MB dye molecules from aqueous solution.
- The optimal contact time for the adsorption of MB dye molecules was 15 minutes under operating conditions.
- Langmuir isotherm model was found to fit the equilibrium data very well, with (R^2) equaled to 0.982 for the adsorption of MB.
- Using the Langmuir equation, the maximum adsorption capacity of CKD adsorbents for MB dye was found to be 34.48 mg/g.
- The adsorption kinetics were found to follow the pseudo-second-order rate kinetic model, with a good correlation (R^2) equal to 0.988 for MB.
- The rate-limiting step was a chemosorption type of adsorption.
- For economic issues, CKD wastes proved to be an effective adsorbent and can be applied for removing water coloring MB dye pollutant from wastewater at the same time; it is considered a value-added product valuable for hazardous waste disposal in waterways.

References

[1] K Mohantry, J.T. Naidu, B.C. Meikap, & M.N. Biswas, "Removal of Crystal Violet from Wastewater by Activated Carbons Prepared from Rice Husk," *Ind. Eng. Chem. Res.,* Vol 45, pp. 5165-5171, 2006.

[2] B. Yasemin, & A. Haluk, "Kinetic and Thermodynamic Study of Methylene Blue Adsorption on Wheat Shells," *Desalination*, Vol. 194, pp. 259–267, 2006.

[3] A.S. Al-Zaydien, "Adsorption of Methylene Blue from Aqueous Solution onto a Low-Cost Natural Jordanian Tripoli," *Am. J. Environ. Sci*., Vol. 5, pp. 197–208, 2009.

[4] D. Ozer, G. Dursun, & A. Ozer, "Methylene Blue Adsorption from Aqueous Solution by Dehydrated Peanut Hull," *J. Hazard Mater.*, Vol. 144, pp. 171-179, 2007.

[5] A. zourro, M. Fidaleo, & R. Lavecchia, "Response Surface Methodology (RSM) Analysis of Photo-degradation of Sulfonated Diazo Dye Reactive Green 19 by UV/H_2O_2 Process,".*J..Environ. Mange.* ln Press. https://doi.org/10.1016/j.jenvman, 2013.

[6] A. Caselatto, J.F. Ferrari, B.E. Tambourgi, R. Moraes, & E. Silveira, "Biodegradation of Textile Azo Dyes by Shewanella Putrefaciens (CCT 1967), *Chemical Engineering Transactions*, Vol. 24, pp. 871–876, 2011.

[7] K. Batheja, A. K. Sinha & G. Seth, "Studies on Water Treatment for Removal of Nitrate," *Asian J. Exp. Sci.*, Vol. 23, No. 1, pp. 61-66, 2009.

[8] P. M. Ayyasamy, S. Rajakumar, M. Sathishkumar, K. Swaminathanc, K. Shanthi, P. Lakshmanaperumalsamye, & S. Lee, "Nitrate Removal from Synthetic Medium and Groundwater with aquatic Macrophytes," *Desalination*, Vol. 242, pp. 286-296, 2009.

[9] A. Kapoor & T. Viraraghavan, "Nitrate Removal from Drinking Water: A_Review," *J. Environmental Engineering*, Vol. 123, No. 4, pp. 371-380, 1997.

[10] A. Afkhami, "Adsorption and Electro-sorption of Nitrate and Nitrite on High-Area Carbon Cloth: An Approach to Purification of Water and Wastewater Samples," *Letters to the Editor /Carbon*, Vol. 41, pp. 1309-1328, 2003.

[11] W.T. Tsai, C.Y. Chang, M.C. Lin, S.F. Chien, H.F. Sun, & M.F. Hsieh, "Adsorption of Acid Dye onto Activated Carbons Prepared from Agricultural Waste Bagasse by ZnCl2 Activation," *Chemosphere.*, Vol. 45, pp. 51-58, 2011.

[12] B. Amit, & A.K. Minocha, "Conventional and Non-Conventional Adsorbents for the Removal of Pollutants from Water – A Review." *Indian J. Chem. Tec.*, Vol. 13, pp. 203-217, 2006.

[13] J.A. Abudaia, et al. "Assessment of Activated Carbon Prepared from ate Stones in Adsorption of Indoor Radon." *Al-Nawah J.*, Tajoura Nuclear Research Center. The Libyan Atomic Energy Establishment, Tripoli, Libya, Vol. 11, No. 15, pp. 33-42, 2014.

[14] E.H. Amjed, N.P. Alan, A.K. Hafid, P. Suki, & C. Neil, "Characterization of Activated Carbon Prepared from a Single Cultivar of Jordanian Olive Stones by Chemical and Physiochemical Technique." *J. Anal. App. Pyrolysis*, Vol. 71, pp. 151-164, 2004.

[15] J.A. Jamal, A.S. Ahlam, A.A. Omaima, "Used Tea Leaves as a Low-Cost Adsorption Material for Treating Colored Aqueous Solutions with Dyes," *First Conference on Marine and Groundwater Pollution,* February 20-23, 2018, Tripoli, Libya.

[16] A.N. Souad, "Utilizing Ground Coffee Waste as An Adsorbent for Removing Organic Dyes from Aqueous Media," *A study submitted in partial fulfillment of the requirements for the Master of Science degree in Chemistry*, 2018, Libyan Academy for Graduate Studies, Janzour, Tripoli, Libya.

[17] L. Xiamin, T. Yang, C. Xiuju, I. Dandan, I. Fang, & S. Wenjing, "Preparation and Evaluation of Orange Peel Cellulose Adsorbents for Effective Removal of Cadmium, Zinc, Cobalt, and Nickel," *Colloids and Surface A: Physiochem. Eng. Aspects*, Vol. 317, pp. 512-521, 2008.

[18] P. Erol, A. Turkan, & P. Serife, "Utilization of Barley Straws as Biosorbents for Cu2+ and Pb2+ ion," *J. Hazard. Mater.*, Vol. 164, pp. 982-986, 2012.
[19] P.L. Ashly, & S. Thirumalisamy, "Adsorption of Hazardous Cationic Dyes from Aqueous Solution onto Acacia Nilotica Leaves as an Eco Friendly Adsorbent," *Sustain. Environ. Res.*, Vol. 22, No. 2, pp. 113-122, 2012.
[20] F. Deniz, & S. Karaman, "Removal of Basic Red 46 Dye from Aqueous Solution by Pine Tree Leaves," *Chem. Eng. J.*, Vol. 170, pp. 67-74, 2011.
[21] S.M. Sabry, D.S. Aly, & M.S. Farahat, "Removal of Heavy Metals from Aqueous Solution by Zeolite in Competitive Sorption System," *Inter. J. Environ. Sci. and Develop.*, Vol. 3, No. 4, pp. 362-367, 2012.
[22] W. Nasira, I. Muhammed, M. Akhtar, S. Muhammed, & W. Amir, "Synthesis, Characterization, and Applications of Silk/Bentonite Clay Composite for Heavy Metal Removal From Aqueous Solution," *Front. Chem.*, Vol. 7, pp. 654, 2019, doi: 10.3389/fchem.2019.00654
[23] K.P. Amid, R.R. Krishna, & M. Kranti, "Removal of Nickel and Phenanthrene from Kaolin Soil Using Different Extractants," *Environ. Eng. Sci.*, Vol. 21, No. 6, 2004, https://doi.org/10.1089/ees.2004.21.691
[24] K. Chiranjeevil, K.M. Radha, M.S. Vineeshal,, & T.N. Bala, "Fly Ash for Removal of Malachite Green Dye from Wastewater: Kinetics and Isotherm Studies," *J.Sci. Technol.*, Vol. 5, No. 3, pp. 195-204, 2020.
[25] D. Claveau-Mallet, W. Scott & C. Yves "Removal of Phosphorus, Fluoride and Metals from a Gypsum Mining Leachate Using Steel Slag Filters." *Water Research J.*, Vol. 47, No. 4, pp. 1512-1520, 2013.
[26] M. El Zayat, E. Sherien & E. Salah, "Characterization of Cement Kiln and Slaked Limestone for Potential Usage in Treatment Studies of Domestic wastewater," *Proceeding of the 6th International Perspective on Water Resources and Environment,* 2013 by the Environment and Water Resource Institute of the American Society of Civil Engineering (EWRI/ASCE).
[27] S.K. Devi, V.V. Lakshmi, & A. Alakanandana, "Impact of Cement Industry on Environment: An Overview," *Asia Pacific Journal of Research*, Vol. 6, pp. 156-161, 2017.
[28] P.H. Muller, "What is Dust? Characterization and Classification of Kiln Dust." *24th Technical Meeting HolderBank Management and Consulting Ltd.*, Technical Center, Material Division, Aargua, Switzerland, Report No. MA 77/2505/E, 1977.
[29] J.G. Hawkins, I.J. Bhatty, & T.A. Ohare, "Cement Kiln Dust Production, Management and Disposal." R & D Serial No. 2327, Portland Cement Association, 2003, Skokie, Illinois.
[30] A. Hamied, S. Nabila, A. Essam, S. Hamdy, & A.M. Abdelzaher, "Environmental Safe Disposal of Cement Kiln Dust for the Production of Geopolymers," *Egypt. J.Chem.*, Vol. 64, No. 12, pp. 7529-7537, 2021.
[31] N. Aleksandar, K. Vladislav, T. Mihail, T. Liliya, & J.B. Nicolai, "Characterization of Cement Kiln Dust from Bulgarian Cement Plants," *Journal of Chemical Technology and Metallurgy (JCTM)*, Vol. 60, pp. 455-463, 2025.
[32] S.S.P.L.Panagoda, T.H.A.R.Sandeepa, T.VA.W. Perera, I.M.D. Sandunika, T.G.M.S. Siriwardhana, D.S.K.M. Alwis, & S.H.S. Dilka., "Cement Manufacturing Process and its Environmental Impact." *J. Res. Techol. Eng.,* Vol. 4, No. 3, pp. 161-168, 2023.
[33] A.A. Elbaz, M.A. Aboulfotoh, M.A. Dohdoh, & M.A. Wahba, "Review of Beneficial Uses of Cement Kiln Dust (CKD), Fly Ash (FA) and their Mixture," *J. Mater. Environ. Sci.*, Vol. 10, pp. 1062-1073, 2019.
[34] G. Gouamid, R.M. Ouahrani, & B.M. Bensaci, "Adsorption Equilibrium, Kinetics and Thermodynamics of Methylene Blue from Aqueous Solution Using Palm Leaves," *Energy Procedia*, Vol. 36, pp. 898-907, 2013.
[35] L. Ridha, B. Anouar, H. Amor, & H.B. Hameed, "Coffee Waste as Potential for the Removal of Basic Dyes from Aqueous Solution," *Korean J. Chem. Eng.,* Vol. 31, pp. 2198-2206, 2014.
[36] N. Shehata, M. S. Geundi, E.A. Ashour, & R.M.A. Abobeah. "Structural Characteristics of the Egyptian Clay as a Low-Cost Adsorbent," *Int. J. Chem. Process Eng. Res.*, Vol. 3, pp. 35–45, 2016. https://doi.org/10.18488/journal.65/2016.3.2/65.2.35.45
[37] T. Reddy, & L. Reddy, "Spectroscopic Characterization of Bentonite," *J. Lasers, Opt. Photonics*, Vol. 4, pp. 171, 2017. https://doi.org/10.4172/2469-410x.1000171
[38] K. Chinoune, K. Bentaleb, Z. Bouberka, A. Nadim, & U. Maschke. "Adsorption of Reactive Dyes from Aqueous Solution by Dirty Bentonite," *Appl. Clay Sci.*, Vol. 123, pp. 64 – 75, 2016. https://doi.org/10.1016/j.clay.2016.01.006
[39] A.A. El-Refaey, "Investigation of Copper Removal from Aqueous Solution by Cement Kiln Dust as Industrial By-Product," *Alexandria Sci. Exch. J.*, Vol. 38, pp. 149–158. 2017. https://doi.org/10.21608/ASEJAIQJSAE.2017.2455
[40] I.S.E.M. Saraya, & M.E.S. Aboul-Fetouh. "Utilization from Cement Kiln Dust in Removal of Acid Dyes," *Am. J. Environ. Sci.* Vol. 8, pp. 16–24, 2012. https://doi.org/10.3844/ajessp.2012.16.24
[41] A.A. El-Refaey, & S.G.Mohamed. "Removal of Lead from Aqueous Solutions Using Cantaloupe Peels as a Biosorbent vs. Cement Kiln Dust as an Industrial By-Product," *Desalin. Water Treat.*, Vol. 166, pp. 62–71, 2019. https://doi.org/10.5004/dwt.2019.24626
[42] S. Eslam, S.A. Wagih, E.M. Abdel-Ghaffar, M. Waffa & M.E. El-Rafey, "The Effective Treatment of Dye-Containing Simulated Wastewater by Using the Cement Kiln Dust as an Industrial Waste Adsorbent," *Scientific Reports*, 2024, Vol. 14:14589 | https://doi.org/10.1038/s41598-024-64191-5
[43] J.S. Hossam, "Adsorption of Methyl Red from Aqueous Solution Using Activated Carbon Prepared from Coffee Residue," *Inter. J. Environ.*, Vol. 3, No. 2, pp. 126-132, 2010.
[44] H. Hameed, K. Mahmoud, & I. Ahmed, "Sorption of Basic Dye from Aqueous Solution by Pommel Peel in a Batch System," *Colloid Surface* A., Vol. 316, pp. 78-84, 2008.
[45] P. Satish, D. Vaijanta, R. Sameer, & P. Naseem, "Kinetics of Adsorption of Crystal Violet from Aqueous Solution Using Different Natural Materials." *Inter. J. Environ. Sci.*, Vol. 1, No. 6, 2011. ISSN 0976-44023.
[46] K.V. Cupta, "Application of Low-Cost Adsorbents for Dye Removal – A Review," *J. Environ. Mang.*, Vol. 90, pp. 2313-2342, 2009.
[47] S. Bharathi, & P. Ramesh, "Equilibrium, Thermodynamic & Kinetics Studies on Adsorption of Basic Dye by Citrulus Lanatus Rind," *Iran. J. Ener. & Environ. Sci.*, Vol. 1, No. 6, pp. 23-24, 2012.
[48] A.F. Batzias, & K.D. Sidras, "Dye Adsorption by Calcium Chloride Treated Beech Sawdust in Batch and Fixed-Bed Systems," *J. Hazard. Mater.*, B, Vol. 114, pp. 167-174, 2004.
[49] G. ANNADURAL, S. JUANG, & J. LEE, "USE OF CELLULOSE-BASED WASTES FOR ADSORPTION OF DYES FROM AQUEOUS SOLUTIONS," *J. HAZARD. MATER.* VOL. 92, PP. 263-274, 2002.
[50] V. Ponnusami, V. Gunasekar, & N. Srivastav, "Kinetics of Methylene Blue Removal from Aqueous Solution Using Gulmohar (Detonix regia) Plant Leaf Powder: Multivariate Regression Analysis," *J. Hazard. Mater.* Vol. 169, pp. 119-127, 2009.
[51] S. Sener, "Use of Solid Wastes of the Soda Ash Plant as an Adsorbent for the Removal of Anionic Dyes: Equilibrium and Kinetics Studies," *Chem. Eng. J.*, Vol. 138, pp. 207-214, 2008.
[52] L.S. Oliveira, A.S. Franca, M. Alves, & F. Rocha, "Evaluation of Untreated Coffee Husks as Potential Bio-Sorbent for Treatment of Dye Contamination Water," *J. Hazard. Mater.*, Vol. 155, pp. 507-512, 2008.